Particle Simulation of Electrodeless Plasma Thruster with Rotating Electric Field

IEPC-2015-474p／ISTS-2015-b-474p

Presented at Joint Conference of 30th International Symposium on Space Technology and Science
34th International Electric Propulsion Conference and 6th Nano-satellite Symposium,
Kobe, Japan
July 4–10, 2015

Dai Uchigasaki* and Naofumi Ohnishi†
Tohoku University, Sendai, Miyagi, 980-8579, Japan

Two-dimensional particle-in-cell simulations in an acceleration area were conducted with a weakly-penetrating rotating electric field (REF) for examining feasibility of electrodeless propulsion scheme by the REF. In the simulations without a radial magnetic field, negative azimuthal currents appear at a low-voltage electrode side because electrons can feel the REF in this region. For trying to utilize the motion of the electrons in the outer edge, the most effective phase difference of input power voltages was found as making the counter-REF against the original concept of the Lissajous acceleration. Applying the counter-REF to the plasma, we can obtain an outwrd electric field that is generated by the plasma itself especially in a large density-gradient. A thrust produced by the outward electric field and a converging magnetic field could result in 0.1 mN even if we use the practical parameters.

Nomenclature

$\boldsymbol{B}$	= magnetic field vector
B_r	= radial component of magnetic field
B_z	= axial component of magnetic field
B_{z0}	= axial component of magnetic field at $r = 0$
Δt	= time step
Δx	= grid width
e	= elementary charge
$\boldsymbol{E}$	= electric field vector
f	= AC frequency
F	= thrust
$\tilde{F}$	= time averaged thrust
J_θ	= azimuthal current density
$\tilde{J}_\theta$	= time averaged azimuthal current density
$\langle \tilde{J}_\theta \rangle$	= time-space averaged azimuthal current density
k	= Boltzmann constant
l	= index of super-particle
L_0	= distance between a pair of antennae
m	= particle mass

*Graduate Student, Department of Aerospace Engineering, uchigasaki@rhd.mech.tohoku.ac.jp
†Associate Professor, Department of Aerospace Engineering, ohnishi@rhd.mech.tohoku.ac.jp

m_e	= electron mass
n	= number density weight of super-particle
q	= particle charge
r	= radial distance
r_0	= inner radius of glass tube
t	= time
$T_{0,e}$	= initial electron temperature
v_e	= electron velocity
v_z	= axial velocity of super-particle
$\boldsymbol{v}$	= super-particle velocity
V_0	= AC amplitude
z_0	= distance from magnetic dipole
β	= plasma density gradient
ϵ_0	= permittivity of vacuum
$\mathcal{E}$	= penetration level of external electric field
ϕ	= electrostatic potential
ψ	= phase difference of input voltage
ω	= AC angular frequency ($=2\pi f$)
ω_{ce}	= electron cyclotron frequency
ω_{pe}	= plasma frequency

I. Introduction

Space missions for asteroid sample return and satellite attitude control are operated during a long term; e.g., the Hayabusa explorer successfully accomplished a sample return mission that lasted to seven years.[1] An electric propulsion system is therefore necessary to keep supplying thrust power to a spacecraft in such a long-term space mission. However, conventional electric propulsion systems have some problems for longer and deeper space missions because their lifetimes are limited by electrode erosion and contamination due to direct contacts of high-energy plasma particles.[2] An electrodeless electric propulsion system utilizing a dense helicon plasma has been proposed as a solution omitting the plasma contact coupling with some additional acceleration schemes.[3] An acceleration scheme with a rotating electric field (REF) is one of them and is called Lissajous acceleration.

A cross section of an acceleration area of the REF schematically shown in Fig. 1. The acceleration area is located in a downstream side from a helicon plasma source. Two pairs of deflection plate antennae inducing the REF are insulated by a glass tube for preventing the direct contacts of the plasma. A static diverging magnetic field is also externally applied in the acceleration area. The plasma creates an azimuthal current J_θ because $\mathbf{E}\times\mathbf{B}$ drift motion is induced by the REF and an axial component of the diverging magnetic field B_z. An axial Lorentz force is then produced by J_θ and a radial component of the diverging magnetic field B_r; i.e., the plasma accelerates to the axial direction. Note that the diverging magnetic field has another role as making a magnetic nozzle.[4]

Although the Lissajous acceleration has been experimentally investigated, any clear indication of the electromagnetic acceleration has never found yet.[6] Moreover, previous numerical works suggested that the REF did not sufficiently penetrate into the dense helicon plasma nor create the $\mathbf{E}\times\mathbf{B}$ drift motion[5] in the past experiments. Penetration level of the external REF is theoretically predicted as follows;[7]

$$\mathcal{E} = \frac{2}{\zeta}(\sqrt{1+\zeta} - 1), \tag{1}$$

$$\zeta = \frac{8e\omega_{pe}^2}{m_e\omega^2\omega_{ce}^2 L_0}\frac{2V_0}{L_0}. \tag{2}$$

The feasible value of $\mathcal{E}$ in experiments is much less than 0.5, though the plasma ideally rotates only with $\mathcal{E} > 0.6$.[5] The plasma motion is not analytically expectable because it is affected just near the edge by such a weakly-penetrating electric field and charge distribution becomes highly nonuniform. Actually, the counter-rotating plasma was found with the weakly-penetrating REF in the previous numerical study,[5] which cannot be explained by an analytical prospect.

Numerical simulations help us to understand the plasma motion in the acceleration area even with the non-ideal penetration condition and may provide another aspect for the plasma acceleration using the REF. We therefore conducted two-dimensional particle-in-cell (PIC) simulations in order to analyze the plasma motion in a cross section of the acceleration area and examined a feasibility of the plasma acceleration with a weakly-penetrating REF.

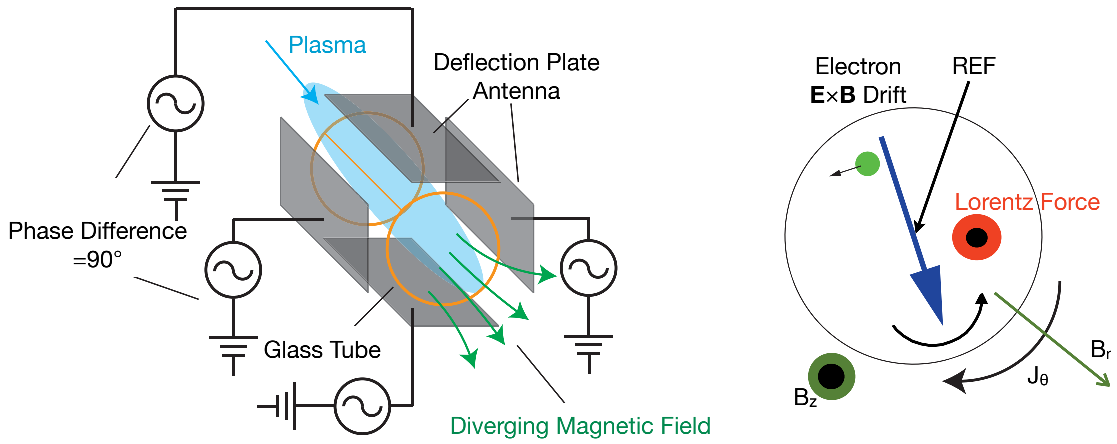

Figure 1. Schematic view of the electrodeless electric propulsion with the REF.

II. Numerical Methods and Conditions

We employ the two-dimensional electrostatic PIC method.[8] Basic equations for the particle motion and electric field are given by

$$m\frac{d\mathbf{v}}{dt} = q(\mathbf{E} + \mathbf{v} \times \mathbf{B}), \tag{3}$$

$$\nabla \cdot (\epsilon_0 \nabla\phi) = -\rho, \tag{4}$$

$$\mathbf{E} = -\nabla\phi. \tag{5}$$

In this method, ions and electrons are treated as super-particles consisting of many actual particles. We give a finite size to super-particles and distribute their charge to each grid point with a weighting method in order to compute the charge density at the grid point. The Poisson's equation (4) for the electrostatic potential ϕ is solved with the charge density calculated by the particle distribution, and the electric field is obtained from Eq. (5). The super-particles move under the influence of this self-consistent electric field by following Eq. (3). A static magnetic field is only considered in this study because the induction component could be much smaller than the the external field and thus generates a negligible current.

Two dimensional-simulations were carried out in a cross section of the acceleration area as shown in Fig. 2. This domain covers a 2.4 × 2.4 cm^2 square, and the plasma is surrounded by a circular dielectric wall to mimic a glass tube used in the experiments.[9] The inner diameter of the circular tube is 2.0 cm, and the thickness is 0.2 cm. Two pairs of the deflection antennae are 1.6 cm in length and are located at each boundary. The applied AC voltages are given by sinusoidal functions with phase differences. The top and bottom antennae are biased by $\pm V_0 \sin(\omega t + \psi)$, while the left and right are $\pm V_0 \sin(\omega t)$. We assumed a magnetic dipole potential to express the diverging magnetic field in the two-dimensional domain, which is defined by

$$B_z(r) = \frac{z_0^3}{2}\frac{2z_0^2 - r^2}{(r^2 + z_0^2)^{\frac{5}{2}}} B_{z0}, \tag{6}$$

$$B_r(r) = \frac{z_0^3}{2}\frac{3rz_0}{(r^2 + z_0^2)^{\frac{5}{2}}} B_{z0}. \tag{7}$$

The helicon plasma is assumed to be composed of argon ions and electrons, and their initial temperatures are 0.5 eV and 5 eV, respectively. Collisions with the neutral particles are not included in this study because they have only a minor contribution to the plasma motion.[10] The initial positions of the super-particles are distributed by weighted random numbers to form the initial density distribution of

$$n_p(r) = n_{p0}\left\{1 - \beta\left(\frac{r}{r_0}\right)^2\right\}. \tag{8}$$

We set the grid size Δx to be smaller than the Debye length and the time step Δt to smaller than 0.1 times of the plasma frequency. If the charged particles reach a dielectric wall, they are diffusively reflected, that is, redefined with the thermal velocity based on the wall temperature of 300 K to describe loss of particles momenta.

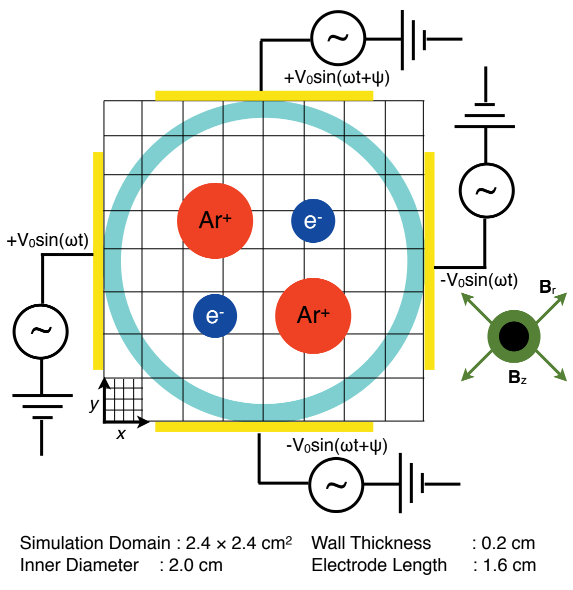

Figure 2. Simulation conditions.

III. Results and Discussions

III.A. Electron motions in a weakly-penetrating electric field

The simulations were first carried out without the radial magnetic component B_r under the condition of the uniform axial component $B_z = B_{z0}$. Figure 3 shows the time-space-averaged current densities in the azimuthal direction $\langle \tilde{J}_\theta \rangle$ as a function of B_z in a weakly-penetrating electric field ($\mathcal{E} < 0.5$). Although small-absolute azimuthal currents are obtained for large B_z, $\langle \tilde{J}_\theta \rangle$ takes large-absolute negative values with decreasing of B_z and a transition is found around $B_z \sim 0.03$ T that corresponds to the condition of $\omega_{ce} \sim \omega_{pe}$.

Figure 4 shows the spatial distributions of J_θ under the condition for which the electron cyclotron frequency is less than the plasma frequency. Purple arrows in the left panel represent the direction of the electrons motion at the plasma edge where the J_θ gives a negative value, while the green arrows denote the electric field direction at each timing. When $\omega_{ce} < \omega_{pe}$, the electrons are difficult to be restricted by the magnetic field lines and an electric potential created by the plasma is higher than that at the dielectric wall, resulting in a sheath formation. A strong electric field therefore appears especially in the negative voltage side. As a sequel to the strong field at the outer edge, the electrons accelerate to the same circumferential direction and yield a large-absolute negative $\langle \tilde{J}_\theta \rangle$.

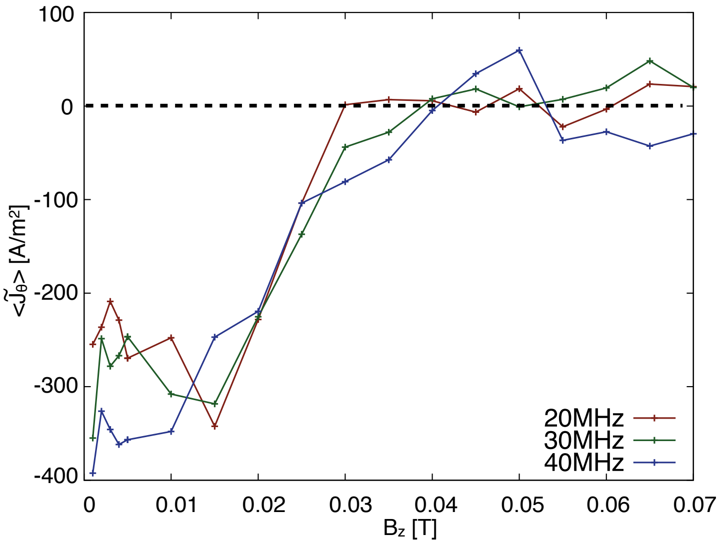

Figure 3. Space-time-averaged azimuthal current $\langle \tilde{J}_\theta \rangle$ under the condition of the weakly-penetrating REF ($n_{p0} = 10^{10}$ cm $^{-3}$, $V_0 = 500$ V).

We next focus on the negative J_θ to accelerate electrons with a converging magnetic field since the large-absolute values are stably obtained with a weakly-penetrating REF. The PIC simulations for estimating the axial thrust included the radial component of the magnetic flux density B_r representing the converging field. The axial thrust F from the two-dimensional simulation is estimated as follows;

$$F = \sum_l (n_l |v_{z,\,l}|) m_l v_{z,\,l}. \tag{9}$$

Time-averaged thrust $\tilde{F}$ is calculated by averaging F for five periods except the first period.

Figure 5 shows the time-averaged thrust $\tilde{F}$ against the parameter β which determines the initial density gradient of the plasma (see Eq. (8)). No significant thrust under this condition suggests that the azimuthal current presenting in the sheath region is not enough to produce the axial thrust. Although we found the parameters for getting electrons rotational stream with the weakly-penetrating REF, they dose not result in a significant thrust.

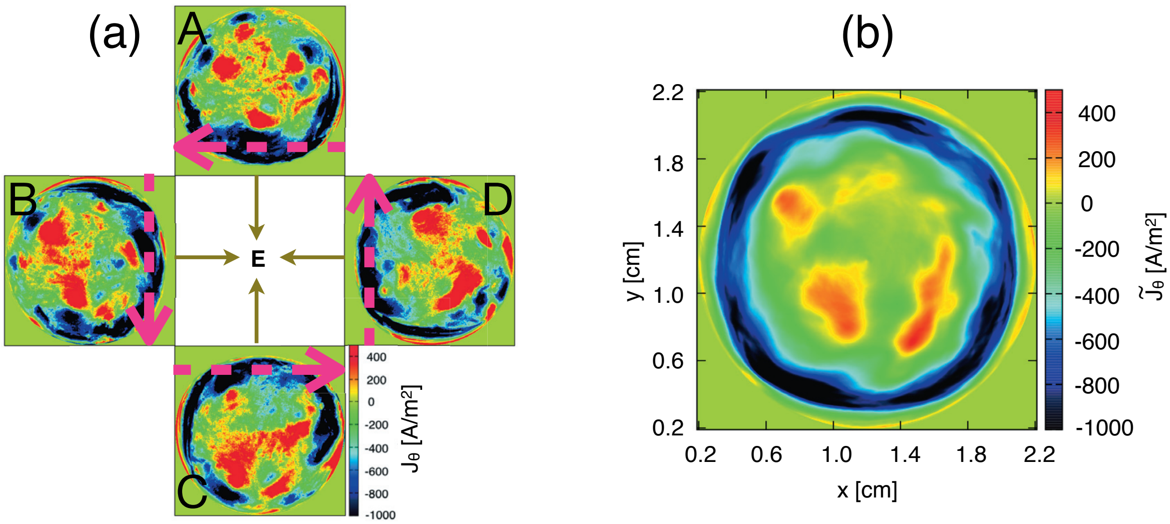

Figure 4. Contours of J_θ (a) at each quarter cycle of the REF and (b) its time-averaged value ($n_{p0} = 10^{10}$ cm^{-3}, $V_0 = 500$ V, $f = 30$ MHz, $B_{z0} = 0.016$ T).

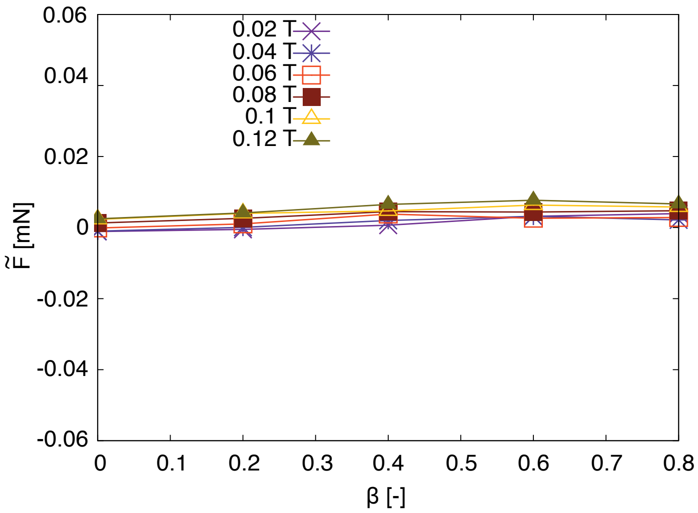

Figure 5. Relation between $\tilde{F}$ and β ($n_{p0} = 10^{11}$ cm^{-3}, $V_0 = 1,500$ V, $f = 100$ MHz).

III.B. Effect of phase difference among applied voltages

The original concept of the Lissajous acceleration expects the $\boldsymbol{E} \times \boldsymbol{B}$ drift motion following the REF. However, the counter-rotating drift appears with the weakly-penetrating REF and now makes no sense in the rotational direction of the electric field. We examined the optimum rotational direction of the REF, that is, the phase difference of the applied voltage for a larger thrust. Figure 6 shows the dependence of the averaged kinetic energy of electrons on the phase difference ψ without radial magnetic field component. The averaged kinetic energy of electrons has a peak at $\psi = 270°$ and is higher than the ordinary cases with $\psi = 90°$ shown above. Here, $\psi = 90°$ means that the electric field rotates in counter-clockwise in Fig. 4, on the other hand $\psi = 270°$ means the clockwise rotation. For the case of $\psi = 90°$, the electrons move in a sequence from A, B, C to D in Fig. 4. However, the moving direction on the edge is opposed to the azimuthal currents corresponding to the purple arrows and thus does not give a continuous acceleration. In contrast, for the case of $\psi = 270°$, the electrons move in a sequence from D, C, B to A and continuously accelerate. This is why the phase difference of $\psi = 270°$ produces the largest kinetic energy.

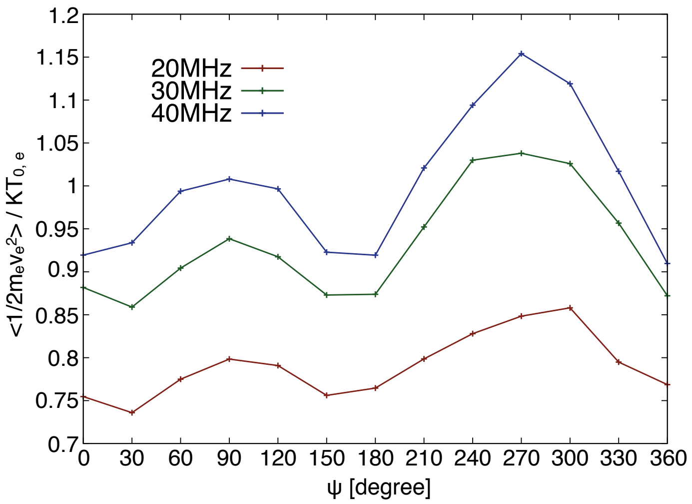

Figure 6. Relation between the averaged kinetic energy of electrons and phase difference ψ ($n_{p0} = 10^{10}$ cm^{-3}, $V_0 = 500$ V, $B_{z0} = 0.016$ T).

In order to estimate the thrust generated by the REF of $\psi = 270°$, we again included B_r into the PIC simulations. Figure 7 shows the averaged thrust $\tilde{F}$ against the density gradient parameter β with $\psi = 270°$. A significant thrust of ~ 0.1 mN is achieved even if we employ the experimental value of $\beta \sim 0.6$.[11] The electron motion is activated with $\psi = 270°$ because the directions of the electron motion and the REF are identical to each other and charge separation appears in a wide region not only the plasma edge.

The charge separation tends to produce an outward electric field since an ion rich region makes a positive electric potential. A large-absolute negative J_θ is induced by the outward electric field and B_z, and the axial thrust is consequently produced by J_θ (< 0) and B_r of the converging magnetic field. The axial thrust $\tilde{F}$ increases as β does because the center of the plasma is likely to bear a positive charge for higher β. For $B_{z0} = 0.2$–0.8 T ($\omega_{ce} < \omega_{pe}$), the axial thrust $\tilde{F}$ increases with B_{z0} because the higher B_{z0} means the higher B_r so that the Lorentz force $J_\theta \times B_r$ becomes larger. For $B_{z0} > 0.8$ T ($\omega_{ce} > \omega_{pe}$), however, $\tilde{F}$ does not follow B_{z0}. This comes from the fact that the electrons stream in the circumferential direction is not effectively induced for $B_{z0} > 0.8$ T so that the charge separation is unlikely to occur.

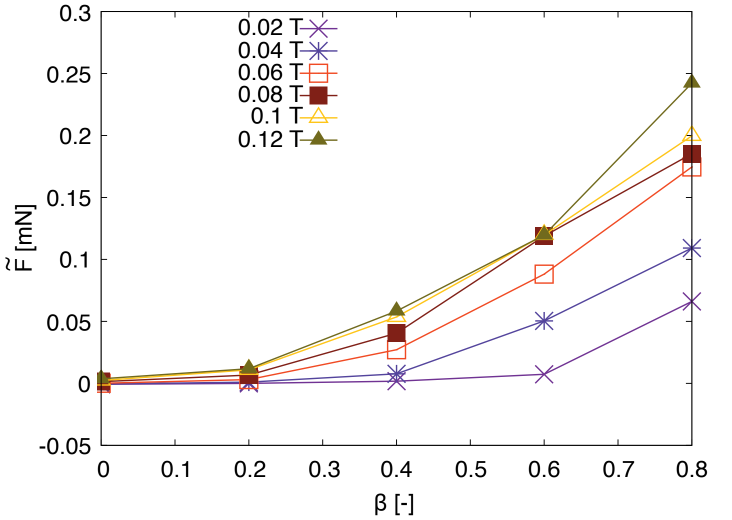

Figure 7. Relation between the axial thrust $\tilde{F}$ and density gradient parameter β with $\psi = 270°$ ($n_{p0} = 10^{11}$ cm^{-3}, $V_0 = 1,500$ V, $f = 100$ MHz).

IV. Conclusion

Two-dimensional PIC simulations were carried out in order to investigate the acceleration with weakly-penetrating REF in the electrodeless plasma thruster. Applying the REF of $\psi = 270°$ and an appropriate magnetic field that satisfies $\omega_{ce} < \omega_{pe}$, energy transfer from the REF energy to the electrons becomes efficient, and the electrons stream in the circumferential direction is induced, producing a large-absolute azimuthal current. The induced electron motion yields a charge separation especially in the nonuniform plasma which has a high central density (e.g., helicon wave plasma) so that an outward electric field is produced. The thrust produced by the outward electric field and converging magnetic field may approach to 0.1 mN in a nonuniform dense plasma of $\beta = 0.6$ and $n_{p0} = 10^{11}$ cm^{-3} even under conditions of the weakly-penetrating REF of $\mathcal{E} < 0.5$.

The acceleration mechanism with the weakly-penetrating REF is suitable for a high-density helicon wave plasma because the experimental plasma density exceeds 10^{13} cm^{-3} and applying a strong magnetic field is possible with $\omega_{ce} < \omega_{pe}$. Three-dimensional simulations, however, are indispensable to confirm the REF acceleration, and the inductive electromagnetic field should be taken into account for the detailed analysis. The REF acceleration scheme for the helicon wave plasma unfortunately does not attribute to the simple Lissajous acceleration as expected earlier but still has a possibility to attain a required thrust for an electrodeless plasma thruster.

References

[1]K. Nishiyama and H. Kuninaka, "Discussion on Performance History and Operations of Hayabusa Ion Engines," Transactions of JSASS, Aerospace Technology Japan, **10**, Tb_1-Tb_8 (2012).

[2]H. Kuninaka et al., "Assessment of Plasma Interactions and Flight Status of the HAYABUSA Asteroid Explorer Propelled by Microwave Discharge Ion Engines," IEEE Transactions on Plasma Science, **34**, 2125 (2006).

[3]S. Shinohara et al., "Development of Electrodeless Plasma Thrusters With High-Density Helicon Plasma Sources," IEEE Transactions on Plasma Science, **42**, 1245 (2014).

[4]E. Ahedo and M. Merino, "Two-dimensional supersonic plasma acceleration in magnetic nozzle," Physics of Plasmas, **17**, 073501 (2010).

[5]R. Nomura et al., "Numerical Study of Lissajous Acceleration for Electrodeless Plasma Thruster," Proceedings of the 33rd International Electric Propulsion Conference, October 2013, IEPC-2013-210 (2013).

[6]T. Matsuoka et al., "Laboratory Model Development of Lissajous Acceleration for Electrodeless Helicon Plasma Thruster," AIAA Paper 2012-3956 (2012).

[7]T. Matsuoka et al., "Progress in Development for Helicon Plasma Thrusters by Use of the Rotating Electric Field,"

Proceedings of the 32^{nd} International Electric Propulsion Conference, September 2011, IEPC-2011-079 (2011).

[8]C. K. Birdsall and A. B. London, Plasma Physics via Computer Simulation, Institute of Physics Publishing, London (2004).

[9]H. Nishida et al., "Preliminary Study on Electromagnetic Plasma Acceleration for Electrodeless Electric Propulsion," Proceedings of the 28^{th} International Electric Propulsion Conference, March 2003, IEPC-03-0168 (2003).

[10]R. Nomura et al., "PIC Simulation of Electrodeless Plasma Thruster with Rotating Electric Field," Proceedings of 28^{th} International Symposium on Rarefied Gas Dynamics, 1431–1436 (2012).

[11]T. Nakamura et al., "Study on Helicon Plasma Lissajous Acceleration for Electrodeless Electric Propulsion," Transactoins of JSASS, Aerospace Technology Japan, **10**, Tb_17-Tb_23 (2012).